Disrupted Subject-Specific Gray Matter Network Properties and Cognitive Dysfunction in Type 1 Diabetes Patients With and Without Proliferative Retinopathy

Eelco van Duinkerken,[1,2,3]* **Richard G. Ijzerman,**[1] **Martin Klein,**[2]
Annette C. Moll,[4] **Frank J. Snoek,**[2,5] **Philip Scheltens,**[6] **Petra J.W. Pouwels,**[7]
Frederik Barkhof,[8] **Michaela Diamant,**[1] **and Betty M. Tijms**[6]

[1]*Diabetes Center/Department of Internal Medicine, VU University Medical Center,*
Amsterdam, The Netherlands
[2]*Department of Medical Psychology, VU University Medical Center, Amsterdam,*
The Netherlands
[3]*Department of Psychology, Pontifícia Universidade Católica, Rio De Janeiro, Brasil*
[4]*Department of Ophthalmology, VU University Medical Center, Amsterdam, The Netherlands*
[5]*Department of Medical Psychology, Academic Medical Center, Amsterdam, The Netherlands*
[6]*Alzheimer Center/Department of Neurology, VU University Medical Center, Amsterdam,*
The Netherlands
[7]*Department of Physics and Medical Technology, VU University Medical Center, Amsterdam,*
The Netherlands
[8]*Department of Radiology and Nuclear Medicine, VU University Medical Center, Amsterdam,*
The Netherlands

◆━━━━━━━━━━━━━━━━━━━━━━━━━━━━━━━━━━━◆

Abstract: *Introduction:* Type 1 diabetes mellitus (T1DM) patients, especially with concomitant microvascular disease, such as proliferative retinopathy, have an increased risk of cognitive deficits. Local cortical gray matter volume reductions only partially explain these cognitive dysfunctions, possibly because volume reductions do not take into account the complex connectivity structure of the brain. This study aimed to identify gray matter network alterations in relation to cognition in T1DM. *Methods*: We investigated if subject-specific structural gray matter network properties, constructed from T1-weighted MRI scans, were different between T1DM patients with (n = 51) and without (n = 53) proliferative retinopathy versus controls (n = 49), and were associated to cognitive decrements and fractional anisotropy, as measured by voxel-based TBSS. Global normalized and local (45 bilateral anatomical regions) clustering coefficient and path length were assessed. These network properties measure how the organization of connections in a network differs from that of randomly connected networks. *Results*: Global gray matter network topology was more randomly organized in both T1DM

patient groups versus controls, with the largest effects seen in patients with proliferative retinopathy. Lower local path length values were widely distributed throughout the brain. Lower local clustering was observed in the middle frontal, postcentral, and occipital areas. Complex network topology explained up to 20% of the variance of cognitive decrements, beyond other predictors. Exploratory analyses showed that lower fractional anisotropy was associated with a more random gray matter network organization. *Conclusion*: T1DM and proliferative retinopathy affect cortical network organization that may consequently contribute to clinically relevant changes in cognitive functioning in these patients. *Hum Brain Mapp 37:1194–1208, 2016.*   © 2015 **Wiley Periodicals, Inc.**

Key words: neuroimaging; graph theory; cognition; small worldness; type 1 diabetes; microangiopathy

◆ ━━━━━━━━━━━━━━━━━━━━━━━━━━━━━━━━━ ◆

INTRODUCTION

Type 1 diabetes mellitus (T1DM) is a chronic metabolic disease, with onset usually in early life. It is characterized by an absolute insulin deficiency, necessitating exogenous insulin therapy to control blood glucose levels. Long-term complications, in particular microvascular complications, including proliferative retinopathy, develop as a consequence of prolonged hyperglycemia [Brownlee, 2001].

Besides microvascular complications, cognitive dysfunction is also associated with T1DM and is characterized by decreased processing speed, mental flexibility, and attentional functioning [Brands et al., 2005; Gaudieri et al., 2008]. These decrements may be present as early as 2 years after diagnosis [Northam et al., 1998] and persist well into adulthood and late life [Brands et al., 2006; van Duinkerken et al., 2012b]. A recent study showed that T1DM is also related to an increased risk of dementia, both vascular and Alzheimer's disease [Smolina et al., 2015]. These cognitive changes are related to chronic hyperglycemic exposure, for which proliferative retinopathy serves as a surrogate marker [Jacobson et al., 2011; Wessels et al., 2008]. It is still unclear, however, how cognitive alterations in this disease are related to cerebral anatomical changes.

So far, studies investigating changes in cortical gray matter in T1DM patients have reported conflicting results [Hughes et al., 2013; Lyoo et al., 2012; Musen et al., 2006; van Duinkerken et al., 2014; Wessels et al., 2006], and so the precise relationship between gray matter volumetric/thickness deficits and cognitive dysfunction remains unclear [Lyoo et al., 2012; Musen et al., 2006; van Duinkerken et al., 2014]. Cognitive functioning depends on brain areas and their connections. Possibly measures that take into account the complex connectivity structure of the brain may provide a better explanation of cognitive dysfunction in diabetes type 1.

Recently, it has become possible to take into account the complex connectivity structure of the brain by representing gray matter morphology as a network (also called a graph). A benefit of a network representation is that it allows for the precise quantification of its connectivity structure with tools of graph theory (for recent reviews see e.g., [Bullmore and Sporns, 2012; Collin and van den Heu-

vel, 2013; Stam, 2010]). In a gray matter network, the nodes represent cortical areas that are connected by edges when they correlate in thickness, volume or surface descriptors across subjects [Bassett et al., 2008; He et al., 2007; Sanabria-Diaz et al., 2010], or when they show structural similarity within a single subject [Tijms et al., 2012; for reviews see [Alexander-Bloch et al., 2013; Evans, 2013]. These patterns have been related to anatomical connectivity by axonal fiber tracts [Bullmore and Sporns, 2012], functional synchronization during development [Collin and van den Heuvel, 2013], and genetic influences [Pezawas et al., 2004]. Across imaging modalities, brain networks typically have a small-world topology. Such an organization of connections provides a trade-off between information processing in specialized clusters and information integration by short path lengths between these clusters [Bullmore and Sporns, 2012; Watts and Strogatz, 1998]. Previous studies have demonstrated that gray matter networks become more randomly organized in illness [Bassett et al., 2008; He et al., 2008; Tijms et al., 2013], and have been related to cognitive impairment in Alzheimer's disease [Tijms et al., 2014], suggesting that they capture pathologically relevant information.

In adult T1DM patients, gray matter networks showed a disrupted organization in comparison with healthy controls [Lyoo et al., 2013]. This suggests that gray matter networks are more sensitive to cortical alterations in adult T1DM patients than volumetric or thickness measures, as the cortical structure is largely unaffected in these same patients [Lyoo et al., 2012]. However, those results could not be related to inter-individual differences in disease variables and cognitive functioning, because the networks were based on a group average. It thus remains unclear whether such gray matter network disruptions are related to cognitive dysfunction and specific disease parameters.

In this study, we investigated whether subject-specific gray matter networks [Tijms et al., 2013], were affected by longstanding T1DM and additionally proliferative retinopathy relative to healthy controls. We expected a more random network topology in T1DM when compared with healthy controls, and that this would be associated with worse cognitive functioning. Clinical, anthropometrical, and demographical determinants of potential gray matter

network disruptions were explored. As an exploration of structural correlates of gray matter networks alterations, the correlation between these networks and white matter fractional anisotropy, measured by diffusion tensor imaging (DTI) was also assessed.

MATERIALS AND METHODS

Participants

This study was conducted in accordance with the Declaration of Helsinki and approved by the medical ethics committee of the VU University Medical Center. Written informed consent was obtained from all participants. This analysis is part of a larger project aimed at determining the effect of T1DM and concomitant proliferative retinopathy, as a marker of cumulative hyperglycemic exposure, on cognitive functioning, brain functioning and structure [van Duinkerken et al., 2012b]. Study design, and in- and exclusion criteria are described in more detail elsewhere [van Duinkerken et al., 2012b]. Briefly, 51 patients with proliferative retinopathy, 53 patients without clinically manifest microangiopathy and 51 matched non-diabetes healthy controls were included. Participants had to be between 18 and 56 years of age, right-handed, and patients had to have T1DM for at least 10 years. Exclusion criteria included psychiatric disorders, history of or current alcohol (men >21; women >14 units a week) or drug use, head trauma, cerebro- or cardiovascular disease, MRI contraindications and centrally acting medication use. For controls, hypertension was an exclusion criterion.

Biomedical and Anthropometric Measures

Blood was drawn to determine Hb/Ht, lipid profile, TSH, liver enzymes, and glycated hemoglobin (HbA1c). Twenty-four hour urine sampling was performed by all patients to determine albumin and creatinine excretion. Proliferative retinopathy was ascertained by fundus photography and rated according to the EURODIAB classification [Aldington et al., 1995]; albuminuria as a 24-h urine albumin:creatinine ratio >2.5 mg/mmol for men or >3.5 mg/mmol for women; neuropathy status was based on the results of the annual check-up patients receive, which is incorporated into the medical records ($n = 92$), or self-report if not available ($n = 12$) [van Duinkerken et al., 2012b]. Lifetime severe hypoglycemic events were self-reported, based on standardized criteria [The Diabetes Control and Complications Trial Research Group, 1996]. Blood pressure was measured three times with 5 min intervals at the left arm in a seated position after a 15-min rest. Hypertension was defined as a mean systolic blood pressure ≥140 mm Hg, a mean diastolic blood pressure >90 mm Hg, or the use of antihypertensive drugs. Depressive symptoms during the past week were evaluated with the Center for Epidemiological Studies Depression scale (CES-D).

MRI Acquisition

MRI scanning was performed on a 1.5 T whole-body MR-system (Siemens Sonata, Erlangen, Germany) using an eight-channel phased-array head coil. For this study a high-resolution T1-MPRAGE (repetition time 2,700 ms, echo time 517 ms, inversion time 950 ms, flip angle 8°, 160 coronal 1.5 mm slices with 1.0 mm in-plane resolution) was used. Diffusion Weighted MR Imaging (DWI; 10 volumes without directional weighting and 60 volumes with 60 noncollinear gradient directions [b value 700 s/mm²]; repetition time 8,500 ms; echo time 86 ms; 59 contiguous axial slices; isotropic 2 mm resolution) was used for white matter fractional anisotropy.

T1-MPRAGE Preprocessing

All scans were corrected for scanner-specific geometric distortions. The origin of the scans was automatically set to the anterior commissure using the linear transformation matrix to Montreal Neurological Institute space calculated in FSL-FLIRT, using 12 degrees of freedom [Jenkinson and Smith, 2001], and subsequently segmented into cerebrospinal fluid, gray and white matter using Statistical Parametric Mapping software (SPM8; Functional Imaging Laboratory, University College London, London, UK) run in MATLAB 7.12 (MathWorks, Natick, MA). Gray matter segmentations were resliced into 2 mm³ isotropic voxels. Ninety anatomical (78 cortical and 12 subcortical) areas were parcelated in each of the native space gray matter segmentations with the Automated Anatomical Labeling Atlas (AAL; [Tzourio-Mazoyer et al., 2002]), and the Individual Brain Atlases Statistical Parametric Mapping (IBASPM; [Alemán-Gómez et al., 2006]) toolbox in SPM8. This toolbox was also used to calculate total intracranial volume, total gray matter volume and the volumes of the AAL regions. To increase robustness of the analysis, the corresponding regions in the left and right hemisphere were averaged to create a bilateral parameter for that region. This way, 45 regions were used in the analyses.

Gray Matter Network Analysis

Gray matter networks were extracted using in-house developed software (https://github.com/bettytijms/Single_ Subject_Gray_Matter_Networks) that was developed in Matlab v7.12.0.635 (for technical details please see Tijms et al. [2012]. Briefly, the nodes were defined as small regions of interest of 3 × 3 × 3 voxels, and nodes were connected by edges with a weight determined by the correlation coefficient that quantified the structural similarity between nodes. Next, networks were binarized at a threshold that was determined so that for all subject-specific

networks the chance of including spurious correlations was approximately 5%, corrected for multiple hypothesis testing using a permutation based method [Noble, 2009]. Nodes within each graph were only connected when their similarity value survived this threshold. We calculated for each node in the network the characteristic path length L (i.e., the minimum number of edges between any pair of nodes) and the clustering coefficient C (i.e., the level of interconnectedness between neighboring nodes). Next, path length (λ) and clustering coefficient (γ) were calculated by averaging the characteristic path length L and clustering coefficient C across the nodes for each graph and then dividing these whole-brain properties by those averaged from 20 randomized reference graphs with an identical size and degree distribution [Maslov and Sneppen, 2002]. Of these 20 random reference graphs, the standard deviation for clustering coefficient ranged between 0.000013 and 0.00014. For path length the standard deviation ranged between 0.0000010 and 0.000020. These small standard deviations and range indicated that 20 random networks were sufficient to obtain stable normalized network properties. This is similar to our previous research also showing that using 20 random reference graphs is sufficient to obtain stable network statistics [Tijms et al., 2013]. When the clustering coefficient is higher than that of a random reference graph of identical size and degree (i.e., $\gamma \geq 1$), and when the path length is similar (i.e., $\lambda \approx 1$) a network has the "small world" property (i.e., $\gamma / \lambda \geq 1$) [Humphries and Gurney, 2008; Watts and Strogatz, 1998]. Previous studies have demonstrated that in neurological and psychiatric disorders the organization of gray matter networks becomes more like that of a random reference graph (i.e., the small world property becomes smaller) [Bassett et al., 2008; He et al., 2008; Tijms et al., 2015; Tijms et al., 2014]. We calculated betweenness centrality (i.e., the proportion of characteristic paths that run through a node) to assess the centrality of nodes. In order to reduce dimensionality of the data and to aid comparability between subject-specific networks, we averaged local graph properties across nodes in 45 bilateral anatomical areas as defined by the AAL atlas. We also computed the graph defining properties size (i.e., the number of nodes), average degree (i.e., the number of edges) and connectivity density (i.e., the number of existing edges to the number of all possible edges) since other types of graph properties are dependent on these [van Wijk et al., 2010]. More technical details of all graph properties and their interpretation have been described by Rubinov and Sporns [2010]. Graph properties were obtained with scripts from the Brain Connectivity Toolbox (www.brain-connectivity-toolbox.net; [Rubinov and Sporns, 2010], which we modified for large networks.

DTI Analysis

DTI processing was previously described in detail in van Duinkerken et al. [2012a]. In short, the FMRIB's Diffu-sion Toolbox (FDT) and Tract-Based Spatial Statistics (TBSS) pipelines of FMRIB's Software Library 4.1 (FSL; http://fsl.fmrib.ox.ac.uk/fsl/fslwiki/) were used to process all DTI-scans and derive fractional anisotropy. Using TBSS, a study-specific white matter skeleton was created, which was thresholded at a FA of 0.2.

Neuropsychological Assessment

Memory, information processing speed, executive functions, attention, motor, and psychomotor speed were tested by means of the Dutch version of the National Adult Reading Test (estimated IQ), Rey Auditory Verbal Learning Test, Wechsler Adult Intelligence Scale, 3rd edition revised Digit Span and Symbol Substitution Test, Stroop Color-Word Test, Concept Shifting Task, Simple Auditory and Visual Reaction Time Tests, Computerized Visual Searching Task, D2-test, Wisconsin Cart Sorting Test, Category Word Fluency Task, Tapping Test and Letter Digit Modality Test (see [van Duinkerken et al., 2009] for more details). Raw scores were transformed into z-scores based on the mean and standard deviation of the healthy controls. If necessary z-scores were transformed so that higher z-values indicated better performance. With the average of these domains the domain general cognitive ability was created.

Statistical Analysis

Subject characteristics, including descriptive graph characteristics (network size, network degree, and connectivity density) were analyzed using one-way ANOVA, Kruskal-Wallis test in the case of non-normality, or χ^2 tests for categorical variables.

Group differences in whole brain network properties (characteristic clustering and path length, betweenness centrality, small-worldness, γ and λ) were investigated with a MANCOVA, correcting for age, sex, systolic blood pressure, depressive symptoms, and gray matter volume. In the case of a significant MANCOVA F-test, individual ANCOVAs for each whole-brain network property were checked for statistical significance. Subsequently, for the statistically significant ANCOVA tests, between-group analyses were performed correcting for multiple comparisons with Bonferroni correction. Cohen's δ was used to determine the effect size of the between-group differences.

Group differences in local bilateral graph properties were investigated with ANCOVAs, correcting for age, sex, systolic blood pressure, depressive symptoms, and gray matter volume. Individual ANCOVAs for each anatomical location were checked for statistical significance after False Discovery Rate (FDR) correction for multiple hypothesis testing. An FDR-corrected P value below 0.05 was considered statistically significant. Subsequently, for the FDR-corrected statistically significant ANCOVA tests, between-group analyses were performed, additionally correcting

for multiple comparisons with Bonferroni correction. The analyses between the three groups were corrected for multiple testing with the Bonferroni method, which is standard in SPSS when covariates are entered into the model. For the analysis of the regional network properties, which are correlated, FDR correction for multiple comparisons was chosen. Here the Bonferroni method would be overly strict. FDR is in this case better suited, although it is still being on the conservative side [Genovese et al., 2002].

Associations between network properties and cognitive functioning were explored with hierarchical, forward, linear regression across all participants. In the first block age, sex, systolic blood pressure, estimated IQ, and depressive symptoms were forced into the model. In the second block, the network parameters that differed between patients and controls were included. To determine biomedical predictors of network properties that differed between patients and controls, linear forward regression was used including as predictors: age, sex, body mass index, mean systolic blood pressure, estimated IQ, depressive symptoms, gray matter volume, diabetes duration, proliferative retinopathy, self-reported lifetime severe hypoglycemic events, HbA1c, albumin:creatinine ratio and total cholesterol. Using FSL's Randomise, correlations between network parameters and fractional anisotropy were explored. Statistical significance was determined at P below 0.05 after FWE-correction.

Statistical analyses were performed with IBM-SPSS20 (IBM-SPSS, Chicago, IL) and FSL-Randomise; R (version 3.0.3, www.R-project.org) was used for FDR correction.

RESULTS

Participant Characteristics

Subject characteristics can be found in Table I. T1-MPRAGE scans of two control participants could not be used due to artifacts. Patients with proliferative retinopathy were older and reported the highest levels of depressive symptoms relative to the other groups. These patients also had higher systolic blood pressure compared with controls (all $P < 0.05$). Relative to patients without, those with proliferative retinopathy had the earliest disease onset age and longest diabetes duration. Also, albumin:creatinine ratio, rates of hypertension and antihypertensive medication use were higher in these patients (all $P < 0.05$). There were no differences in overall gray matter volume. Subject-specific gray matter networks of all groups were of comparable size and degree and all were fully connected (all $P > 0.05$; Table I).

Whole-Brain Network Parameters

The overall MANCOVA F-test was statistically significant between groups ($F_{(2,145)} = 2.189$; $P = 0.003$). Post hoc ANCOVA analysis revealed that, except for betweenness

centrality ($P = 0.703$), all whole-brain network parameters were statistically significant between groups (all $P < 0.05$; Table II; Fig. 1). All subject-specific gray matter networks had a small world topology (i.e. $\gamma/\lambda > 1$; range across all participants 1.36–1.66), but both patient groups showed a more random topology relative to controls (all $P_{\text{bonferroni}} < 0.01$), as indicated by a pronouncedly lower γ and slightly lower λ values in patients (all $P_{\text{bonferroni}} < 0.02$). Clustering and path length were significantly lower in patients with, but not without proliferative retinopathy compared with controls (all $P_{\text{bonferroni}} < 0.02$; Table II; Fig. 1). Patient groups showed similar network property values. The effect sizes of cortical structural network differences between patients and controls were medium to large, and larger for clustering than for path length. An effect size of 0.2 is considered small, of 0.5 medium and 0.8 large [Biessels et al., 2008].

Local Clustering and Path Length

Compared with controls, patients with proliferative retinopathy showed decreased path length in 28 of the 45 bilateral regions (Fig. 2A; Table III). Differences between controls and patients without proliferative retinopathy were seen in the superior medial frontal, middle frontal, superior and inferior orbitofrontal, precuneus, middle temporal, superior and middle occipital and cuneus (all $P_{\text{bonferroni}} < 0.05$; Table III). When patients with proliferative retinopathy were compared with uncomplicated T1DM patients lower path length was found in the pars triangularis, rolandic operculum, supramarginal, superior temporal pole, superior temporal, caudate nucleus, and insula regions (all $P_{\text{bonferroni}} < 0.05$; Table III).

Clustering was shown to be lower in the middle frontal, postcentral, inferior occipital, lingual and fusiform regions in patients with proliferative retinopathy versus controls (all $P_{\text{bonferroni}} < 0.05$; Table IV). In those patients without diabetes-related complications clustering was lower in the inferior occipital and fusiform areas relative to controls, and compared with both groups in the insula (all $P_{\text{bonferroni}} < 0.05$; Table IV). Between patient groups clustering was lowest in those with complications in the middle frontal and postcentral regions (all $P_{\text{bonferroni}} < 0.05$; Table IV).

Exploratory analyses taking into account potential confounding due to earlier disease onset age, longer disease duration and older age, yielded similar results (Tables III and IV).

Association Between Global/Local Network Parameters and Cognition

Lower whole brain network property values were related to lower general cognitive ability, memory, motor speed and to a lesser extent to lower information

TABLE I. Baseline characteristics of patient groups and non-diabetes controls

	Type 1 diabetes with proliferative retinopathy	Type 1 diabetes without proliferative retinopathy	Non-diabetes controls	Overall P value
N	51	53	49	–
Age (yr)	44.5 ± 7.2[a,b]	37.8 ± 9.2	36.7 ± 11.2	<0.001
Sex (men/women; % men)	21/30 (41.2)	20/33 (37.7)	19/30 (38.8)	0.935
Estimated IQ[c]	110.2 ± 13.4	106.9 ± 11.2	108.5 ± 11.7	0.399
Depressive symptoms[d]	8.0 (0–42)[a,b]	5.0 (0–31)	4.0 (0–37)	0.005
BMI (km/m^2)	25.6 ± 4.1	24.8 ± 3.5	24.3 ± 3.5	0.189
A1C (mmol/mol)	64.7 ± 14.1[a]	61.7 ± 9.8[a]	34.2 ± 2.6	<0.001
A1C (%)	8.1 ± 1.3[a]	7.8 ± 0.9[a]	5.3 ± 0.2	<0.001
Systolic blood pressure (mm Hg)	133.6 ± 17.3[a]	129.1 ± 14.7	123.6 ± 11.3	0.004
Diastolic blood pressure (mm Hg)	76.0 ± 8.7	78.2 ± 9.5	77.4 ± 7.2	0.426
Total cholesterol (mmol/l)	4.5 ± 0.7	4.7 ± 0.7	4.5 ± 0.9	0.217
Current smoking (%)	6 (11.8)	10 (18.9)	11 (22.4)	0.371
Cholesterol medication (%)	11 (20.8)	16 (31.4)	–	0.226
Blood pressure medication (%)	32 (62.7)[b]	6 (11.3)	–	<0.001
Hypertension (%)[e]	33 (64.7)[b]	13 (24.5)	–	<0.001
Albumin:creatinine ratio (mg/ mmol; min-max)	0.91 (0–33.17)[b]	0.39 (0–3.19)	–	0.003
BG before MRI (mmol/l)	9.2 ± 3.7	10.5 ± 4.7	–	0.124
BG before NPA (mmol/l)	8.6 ± 4.0	8.4 ± 4.0	–	0.777
Diabetes duration (yrs)	34.3 ± 7.9†	21.6 ± 9.3	–	<0.001
Diabetes onset age (yrs)	10.2 ± 7.2†	16.2 ± 9.7	–	0.001
Diabetes early onset age (%)[f]	18 (35.3)	10 (18.9)	–	0.077
Severe hypoglycemic events (min-max)[g]	2.0 (0–40)	2.0 (0–50)	–	0.701
Neuropathy (%)[h]	25 (49)	–	–	–
Albuminuria (%)[i]	14 (27.5)	–	–	–
Mean global gray matter volume (mm^3)	614.08 ± 81.4	614.97 ± 74.0	639.23 ± 91.0	0.282
Network size[j]	7,473 ± 688	7,439 ± 746	7,591 ± 757	0.994
Network degree[k]	1,102 ± 115	1,108 ± 120	1,151 ± 120	0.356
Connectivity density[l]	14.81 ± 0.68	14.97 ± 0.69	15.24 ± 0.80	0.163

Data are means ± standard deviation, median with minimum and maximum or absolute numbers with percentages. NPA: neuropsychological assessment. BG: blood glucose.

[a]Statistically different from controls.

[b]Statistically different from patients without proliferative retinopathy.

[c]Estimated IQ was measured using the Dutch version of the National Adult Reading Test (NART).

[d]Depressive symptoms were measured using the Center for Epidemiological Studies scale for Depression.

[e]Hypertension was defined as a systolic blood pressure of ≥140 mm Hg, a diastolic blood pressure of ≥90 mm Hg or the user of antihypertensive drugs. Controls with hypertension were excluded from the study.

[f]Diabetes early onset age was defined as an onset age below the age of 7 years.

[g]Severe hypoglycemic events were self-reported and defined as events for which the patient needs assistance from a third person to recuperate as a result of loss of consciousness or seriously deranged functioning, coma, or seizure owing to low glucose levels.

[h]Neuropathy was based on medical records or, in case they were not available, based on self-report.

[i]Albuminuria was defined as an albumin:creatinine ratio >2.5 mg/mmol for men and >3.5 mg/mmol for women.

[j]Size is defined as the number of nodes of a network.

[k]Degree is defined as average number of edges per node.

[l]Connectivity density is defined as the percentage of existing edges out of the total number of possible edges.

processing speed and executive functioning (all $P < 0.05$; Table V). After averaging across the regions that were found to differ between patients and controls, lower local clustering and lower local path length showed similar relationships with decreased cognitive functioning (Table V).

For general cognitive ability the mean path length of all local regions differing between groups explained 14% of the variance beyond the first model (Table VI). For motor speed this was mean clustering of all regions differing between groups, explaining 22% of the variance, and for

TABLE II. Mean values of whole brain network measures with effect size

	Type 1 diabetes with proliferative retinopathy	Type 1 diabetes without proliferative retinopathy	Non-diabetes controls	Mean difference	P value (Bonferroni)	Effect size (Cohen's δ)
Small-worldness	1.48 ± 0.05		1.54 ± 0.06	−0.063	0.004	−1.10 (−1.11 to −1.08)
		1.50 ± 0.06	1.54 ± 0.06	−0.041	0.007	−0.67 (−0.69 to −0.66)
Gamma (γ)	1.59 ± 0.06		1.67 ± 0.08	−0.084	0.016	−1.15 (−1.16 to −1.12)
		1.62 ± 0.07	1.67 ± 0.08	−0.053	0.010	−0.67 (−0.69 to −0.65)
Lambda (λ)	1.073 ± 0.01		1.084 ± 0.01	−0.010	<0.001	−1.11 (−1.11 to −1.11)
		1.079 ± 0.01	1.084 ± 0.01	−0.006	0.004	−0.50 (−0.51 to −0.50)
Clustering	0.42 ± 0.01		0.44 ± 0.02	−0.014	0.010	−1.29 (−1.29 to −1.28)
		0.43 ± 0.01	0.44 ± 0.02	−0.008	0.082	−0.65 (−0.65 to −0.64)
Path length	1.99 ± 0.01		2.00 ± 0.02	−0.014	0.007	−0.64 (−0.65 to −0.64)
		2.00 ± 0.01	2.00 ± 0.02	−0.007	0.087	−0.19 (−0.20 to −0.19)

Data are represented as mean with standard deviation. An effect size of 0.2 is considered small, of 0.5 medium and 0.8 large [Biessels et al., 2008].

psychomotor speed this was lambda, explaining 21% of the variance (λ; all $P < 0.05$; Table VI). For the other cognitive domains no variables were statistically significant in the multivariate models.

Biomedical Predictors of Altered Global/Local Network Parameters

Older age was related to a more random network topology on all variables (Table VII). Higher body mass index was related to a more random network topology on most of the variables and having proliferative retinopathy to a lower mean local path length. Lower global gray matter volume and being male were related to a more random network topology (Table VII).

Associations Between Network Topology and White Matter Fractional Anisotropy

In an earlier study, we did not find statistically significant differences in local volume or thickness in this patient
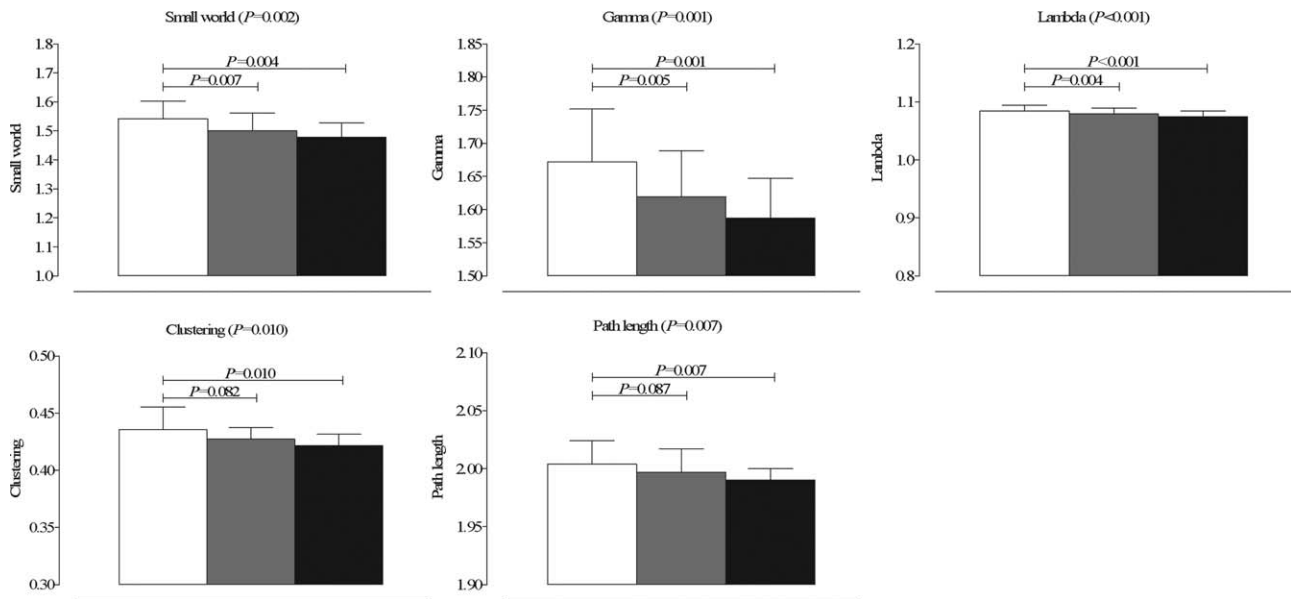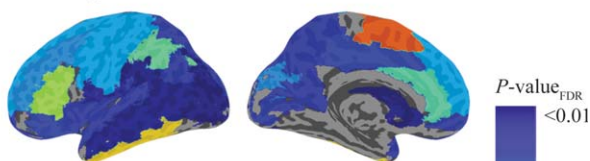

Figure 1.
Bar graph of mean with standard deviation of whole brain network properties that showed differences between both patient groups and controls. White bars indicate non-diabetes controls, gray bars T1DM patients without proliferative retinopathy and black bars patients with proliferative retinopathy.
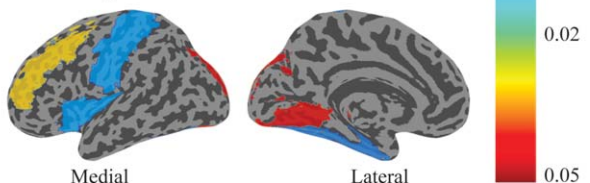
Figure 2.

Schematic representation of the brain regions that show statistically significant differences in path length (**A**) and clustering (**B**) after FDR-correction for multiple comparisons. A) Path length was reduced in patients when compared with controls in the superior, superior medial, and, middle frontal, superior, medial, and inferior orbitofrontal, the supplemental motor area, the pre- and postcentral gyri, rolandic operculum, the superior and inferior parietal, supramarginal, angular gyri, precunei, superior, middle, and inferior temporal and superior temporal pole, the superior and middle occipital, calcarine, and cuneus, the caudate nucleus, anterior and middle cingulum and insula (all $P_{bonferroni} < 0.05$; Table III). B) Clustering was reduced in patients when compared with controls in the middle frontal, postcentral, inferior occipital, lingual and fusiform regions (all $P_{bonferroni} < 0.05$; Table IV). [Color figure can be viewed in the online issue, which is available at wileyonlinelibrary.com.]

sample (van Duinkerken et al., 2014). We therefore explored if white matter fractional anisotropy might provide a mechanism through which network organization is affected. Lower small world values were related to lower fractional anisotropy of the bilateral anterior thalamic radiation and fornix. Together these regions explained 18.6% ($\beta = 0.437$; $P < 0.001$) of the variance of small worldness in this sample (Fig. 3A). The spatial pattern of the association between global clustering and fractional anisotropy was widespread throughout the brain and covered the major white matter tracts bilaterally, including the corpus callosum, thalamic radiation, superior and inferior longitudinal, inferior fronto-occipital and uncinate fasciculi (Fig. 3B). This correlation explained 33.1% ($\beta = 0.579$; $P < 0.001$) of the variance in global clustering. Similar relationships were found for path length, but after correction for confounding factors these lost significance. No negative correlations between network parameters and fractional anisotropy were found.

DISCUSSION

In this study we showed that whole-brain cortical structural organization is more random in T1DM patients with and without proliferative retinopathy relative to healthy controls, as indicated by lower small world values derived from subject-specific cortical networks. At a regional level, lower path length was found throughout the brain, whereas lower clustering coefficient differences were more localized. These alterations were found in both patient groups, albeit patients with proliferative retinopathy showed these alterations in more regions. Moreover, in several of these regions significantly lower path length/clustering was found in patients with versus without proliferative retinopathy. These alterations were associated with age, gray matter volume, body mass index, sex, proliferative retinopathy, and white matter fractional anisotropy. Moreover, worse cognitive functioning was associated with more random network parameters.

A previous study assessed cortical structural organization in T1DM [Lyoo et al., 2013]. Their sample characteristics were similar to our study, but used a group-average approach based on gray matter thickness rather than a subject-specific approach. At a whole-brain level, they observed higher path length values (i.e., loss of global efficiency) and lower clustering coefficient values (i.e., loss of local efficiency) of the gray matter network in T1DM patients, which mostly affected areas involved in executive/control and language functioning. However, this previous study did not compare these values with properties of randomly organized networks. Unnormalized values may be influenced by connectivity density, the number of false positive connections included and/or network size [van Wijk et al., 2010]. In agreement with Lyoo et al. [2013], we also observed loss of clustering, however, we found lower path length values in T1DM patients when compared with controls. We found that a lower clustering coefficient and a lower path length were associated with lower values of the small world properties, and so are suggestive of a more random network organization. We further extended these findings by showing extensive alterations in local path length and locally lower clustering in patients.

Local path length differed between patients and controls in 28 regions. Many of those regions, within the temporal, parietal, cingular and frontal lobes can be considered part of the default mode network [Harrison et al., 2008]. Other regions, such as those in the temporal and frontal cortices are implicated in memory. We also found decreases in the visual cortices and in the (supplementary) motor areas. Local clustering differences were more focal in nature, and mostly found in the visual and motor areas. These latter two findings are, in terms of spatial location, similar to our previous results showing altered motor- and visual resting-state connectivity in this patient group [van Duinkerken et al., 2012b]. Possibly, due to prevalent or subclinical vascular damage of the retina and peripheral nerves, the central areas that are directly connected to the periphery are also affected [van Duinkerken et al., 2012b].

TABLE III. Bilateral regions of significantly altered path length

	Type 1 diabetes with proliferative retinopathy	Type 1 diabetes without proliferative retinopathy	Controls	Overall P_{FDR}-value
Frontal regions				
Superior frontal	1.937 ± 0.017[a]	1.942 ± 0.018	1.946 ± 0.017	0.016
Matched analysis	1.940 ± 0.016	1.936 ± 0.019[a]	1.945 ± 0.018	
Superior medial frontal	1.923 ± 0.022[a]	1.931 ± 0.023[a]	1.943 ± 0.030	0.016
Matched analysis	1.926 ± 0.022	1.924 ± 0.019[a]	1.939 ± 0.032	
Middle frontal	1.961 ± 0.017[a]	1.963 ± 0.015[a]	1.968 ± 0.014	0.014
Matched analysis	1.963 ± 0.017	1.958 ± 0.014[a]	1.967 ± 0.015	
Superior orbitofrontal	1.946 ± 0.020[a]	1.950 ± 0.017[a]	1.959 ± 0.022	0.006
Matched analysis	1.943 ± 0.022[a]	1.949 ± 0.019	1.959 ± 0.023	
Medial orbitofrontal	1.964 ± 0.031[a,b]	1.983 ± 0.035	1.988 ± 0.030	0.006
Matched analysis	1.962 ± 0.032[a]	1.974 ± 0.027	1.986 ± 0.031	
Inferior orbitofrontal	1.964 ± 0.021[a]	1.966 ± 0.017[a]	1.973 ± 0.021	0.008
Matched analysis	1.961 ± 0.021[a]	1.964 ± 0.017[a]	1.973 ± 0.023	
Supplementary motor	1.921 ± 0.021[a]	1.927 ± 0.020	1.934 ± 0.018	0.040
Matched analysis	1.923 ± 0.019	1.922 ± 0.020[a]	1.933 ± 0.019	
Pars triangularis	1.951 ± 0.018†	1.962 ± 0.018	1.959 ± 0.019	0.028
Matched analysis	1.952 ± 0.021	1.958 ± 0.018	1.957 ± 0.019	
Central regions				
Precentral	1.938 ± 0.015[a]	1.941 ± 0.016	1.946 ± 0.012	0.016
Matched analysis	1.940 ± 0.017[a]	1.937 ± 0.015[a]	1.945 ± 0.012	
Postcentral	1.948 ± 0.014[a]	1.952 ± 0.016	1.956 ± 0.014	0.016
Matched analysis	1.948 ± 0.016[a]	1.947 ± 0.016[a]	1.954 ± 0.016	
Rolandic operculum	1.961 ± 0.024[a,b]	1.979 ± 0.025	1.985 ± 0.023	0.003
Matched analysis	1.962 ± 0.025[a]	1.973 ± 0.024	1.982 ± 0.024	
Parietal regions				
Superior parietal	1.948 ± 0.021[a]	1.960 ± 0.018	1.965 ± 0.021	0.006
Matched analysis	1.950 ± 0.020[a]	1.955 ± 0.017[a]	1.964 ± 0.022	
Inferior parietal	1.966 ± 0.019[a]	1.973 ± 0.021	1.979 ± 0.015	0.023
Matched analysis	1.965 ± 0.020[a]	1.966 ± 0.021[a]	1.978 ± 0.016	
Supramarginal	1.950 ± 0.019[a,b]	1.961 ± 0.022	1.965 ± 0.019	0.002
Matched analysis	1.948 ± 0.020[a]	1.954 ± 0.022[a]	1.964 ± 0.020	
Angular	1.965 ± 0.016[a]	1.976 ± 0.021	1.983 ± 0.017	0.006
Matched analysis	1.966 ± 0.017[a]	1.969 ± 0.023[a]	1.982 ± 0.019	
Precuneus	1.967 ± 0.018[a]	1.976 ± 0.018[a]	1.986 ± 0.022	0.006
Matched analysis	1.969 ± 0.019[a]	1.970 ± 0.019[a]	1.985 ± 0.024	
Temporal regions				
Superior temporal pole	1.959 ± 0.020[a,b]	1.972 ± 0.023	1.979 ± 0.023	0.006
Matched analysis	1.959 ± 0.022[a]	1.972 ± 0.025	1.977 ± 0.024	
Superior temporal	1.964 ± 0.016[a,b]	1.975 ± 0.019	1.979 ± 0.020	0.006
Matched analysis	1.962 ± 0.016[a,b]	1.974 ± 0.021	1.977 ± 0.020	
Middle temporal	1.976 ± 0.016[a]	1.981 ± 0.016[a]	1.987 ± 0.018	0.002
Matched analysis	1.975 ± 0.019[a]	1.978 ± 0.018[a]	1.987 ± 0.020	
Inferior temporal	1.979 ± 0.018[a]	1.980 ± 0.018	1.983 ± 0.020	0.033
Matched analysis	1.980 ± 0.021[a]	1.980 ± 0.020[a]	1.984 ± 0.022	
Occipital regions				
Superior occipital	1.946 ± 0.019[a]	1.954 ± 0.020[a]	1.961 ± 0.020	0.006
Matched analysis	1.948 ± 0.022[a]	1.949 ± 0.024[a]	1.960 ± 0.020	
Middle occipital	1.956 ± 0.017[a]	1.962 ± 0.015[a]	1.968 ± 0.014	0.001
Matched analysis	1.956 ± 0.019[a]	1.958 ± 0.014[a]	1.967 ± 0.015	
Calcarine	1.998 ± 0.016[a]	2.008 ± 0.016	2.012 ± 0.013	0.006
Matched analysis	1.996 ± 0.018[a]	2.006 ± 0.017	2.012 ± 0.013	
Cuneus	1.971 ± 0.019[a]	1.974 ± 0.018[a]	1.984 ± 0.018	0.014
Matched analysis	1.973 ± 0.022	1.970 ± 0.018[a]	1.982 ± 0.019	
Subcortical regions				
Caudate nucleus	1.932 ± 0.020[a,b]	1.946 ± 0.018	1.951 ± 0.021	0.001
Matched analysis	1.934 ± 0.019[a]	1.942 ± 0.019	1.950 ± 0.021	

TABLE III. (continued).

	Type 1 diabetes with proliferative retinopathy	Type 1 diabetes without proliferative retinopathy	Controls	Overall P_{FDR}-value
Cingulum				
Anterior cingulum	1.967 ± 0.025^a	1.984 ± 0.027	1.991 ± 0.030	0.023
Matched analysis	1.970 ± 0.027	1.980 ± 0.030	1.989 ± 0.030	
Middle cingulum	1.972 ± 0.018^a	1.983 ± 0.020	1.994 ± 0.025	0.008
Matched analysis	1.972 ± 0.017^a	1.980 ± 0.022^a	1.994 ± 0.027	
Insula				
Insula	$1.987 \pm 0.023^{a,b}$	2.004 ± 0.024	2.007 ± 0.023	0.006
Matched analysis	$1.982 \pm 0.026^{a,b}$	2.000 ± 0.023	2.004 ± 0.024	

Data represent means with standard deviation. In the matched analysis, 27 patient with (mean age: 41.9 ± 7.8; mean disease onset age: 12.9 ± 7.5; mean diabetes duration: 29.0 ± 5.7), 29 patients without proliferative retinopathy (mean age: 40.3 ± 8.9; mean disease onset age: 12.7 ± 8.4; mean diabetes duration: 27.7 ± 8.2) and 38 healthy controls (mean age: 40.8 ± 9.0) were included.
[a]Indicates a statistically significant difference after Bonferroni correction for multiple comparisons between that patient group and controls.
[b]Indicates a statistically significant difference after Bonferroni correction for multiple comparisons between patients with and without proliferative retinopathy.

Cortical network organization was related with individual differences in cognitive functioning. The direction of these associations (lower path length/clustering correlates with poorer cognition) suggests worse cognitive functioning was associated with a more randomly organized network. Global network parameters were associated with speed related domains, which suggests that loss of network efficiency is related to loss of processing speed, a core feature of T1DM-related cognitive dysfunction. The hierarchical regression models showed that motor speed was related to the mean of local clustering, in which the postcentral gyrus is included, a region of major importance for motor functioning. General cognitive ability, which is the mean of all cognitive tests, was related to the

TABLE IV. Bilateral regions of significantly altered clustering coefficient

	Type 1 diabetes with proliferative retinopathy	Type 1 diabetes without proliferative retinopathy	Controls	Overall P_{FDR}-value original analysis
Frontal regions				
Middle frontal	$0.405 \pm 0.018^{a,b}$	0.416 ± 0.018	0.424 ± 0.021	0.034
Matched analysis	$0.403 \pm 0.019^{a,b}$	0.414 ± 0.019	0.423 ± 0.023	
Central regions				
Postcentral	$0.391 \pm 0.020^{a,b}$	0.402 ± 0.018	0.412 ± 0.024	0.015
Matched analysis	0.393 ± 0.021	0.402 ± 0.020	0.411 ± 0.026	
Occipital regions				
Inferior occipital	0.393 ± 0.022^a	0.399 ± 0.022^a	0.414 ± 0.022	0.045
Matched analysis	0.394 ± 0.020	0.397 ± 0.024^a	0.413 ± 0.024	
Lingual	0.348 ± 0.022^a	0.355 ± 0.022	0.368 ± 0.023	0.045
Matched analysis	0.349 ± 0.021	0.355 ± 0.022	0.367 ± 0.025	
Fusiform	0.352 ± 0.021^a	0.359 ± 0.017^a	0.373 ± 0.023	0.014
Matched analysis	0.353 ± 0.021^a	0.356 ± 0.018^a	0.372 ± 0.025	
Insula				
Insula	0.389 ± 0.016	0.389 ± 0.019^a	0.403 ± 0.018	0.015
Matched analysis	0.392 ± 0.016	$0.387 \pm 0.021^{a,b}$	0.401 ± 0.019	

Data represent means with standard deviation. In the matched analysis, 27 patient with (mean age: 41.9 ± 7.8; mean disease onset age: 12.9 ± 7.5; mean diabetes duration: 29.0 ± 5.7), 29 patients without proliferative retinopathy (mean age: 40.3 ± 8.9; mean disease onset age: 12.7 ± 8.4; mean diabetes duration: 27.7 ± 8.2) and 38 healthy controls (mean age: 40.8 ± 9.0) were included.
[a]Indicates a statistically significant difference after Bonferroni correction for multiple comparisons between that patient group and controls.
[b]Indicates a statistically significant difference after Bonferroni correction for multiple comparisons between patients with and without proliferative retinopathy.

TABLE V. Correlations between cognitive domains and global/local network parameters

	General cognitive ability	Memory	Information processing speed	Executive functions	Attention	Motor speed	Psychomotor speed
Mean local clustering	0.193[a]	0.160[a]	0.169[a]	0.116	0.111	0.178[a]	0.001
Mean local path length	0.250[b]	0.236[b]	0.202[a]	0.146	0.135	0.095	0.097
Global clustering	0.191[a]	0.162[a]	0.150	0.138	0.112	0.174[a]	0.016
Global path length	0.190[a]	0.200[a]	0.130	0.129	0.080	0.070	0.106
Small worldness	0.226[b]	0.193[a]	0.158[c]	0.128	0.063	0.201[a]	0.115
Gamma (γ)	0.235[b]	0.208[a]	0.167[a]	0.139	0.074	0.194[a]	0.114
Lambda (λ)	0.241[b]	0.244[b]	0.178[a]	0.169[a]	0.080	0.129	0.088

[a] $P < 0.05$.
[b] $P < 0.01$.
[c] $P = 0.051$.

mean of local path length and psychomotor speed was related to normalized path length (λ). Both functions rely on the integration of various brain regions and thus may explain the relation with more global measures.

The results of the group analyses indicate that alterations in network topology are related to having T1DM per se and are exacerbated by proliferative retinopathy in various regions. The correlation analyses, however, showed that in patients proliferative retinopathy is only related to the mean of local path length and that no other diabetes-related variables (such as disease duration or onset age) were correlated with network parameters. This suggests that other factors related to T1DM might play a role in altered network topology. One possible mechanism may be (neuro)inflammation. Chronic hyperglycemia has been related to an inflammatory response [de Rekeneire et al., 2006]. Indeed, in 37 patients within this study we previously showed elevated levels of peripheral and central macrophage-colony stimulating factor (MCSF; [Ouwens et al., 2014]), which can trigger neuroinflammation by promoting microglial activation [Du Yan et al., 1997]. In an

animal model of T1DM, inflammation has been associated with damage at the cerebral level [Beauquis et al., 2008]. We also found that increased body mass index and more random network topology were related in patients. This provides indirect support that inflammation may be involved, because obesity is known to affect cognition and the central nervous system and is associated with a proinflammatory state [Ownby, 2010; Yates et al., 2012]. Future studies will have to further investigate the contribution of (neuro)inflammation in T1DM-related cerebral compromise.

The regions that showed lower path length and clustering in type 1 diabetes partly coincide with our earlier findings of decreased white matter diffusion properties and altered functional connectivity in this patient group [Demuru et al., 2014; van Duinkerken et al., 2012a,b]. As we did not observe any statistically significant differences in cortical thickness or volume in this group [van Duinkerken et al., 2014], white matter diffusion properties might provide a mechanism through which network organization is affected. Especially global clustering showed a

TABLE VI. Hierarchical regression models of cognitive domains with global/local network parameters

	Model characteristics[a]				Association characteristics		
	Full model adjusted R^2	Adjusted R^2 change[b]	F-value	P	Standardized β	t-value	P
General cognitive ability	0.339	0.014	13.98	<0.001			
Mean local path length					0.145	2.023	0.045
Motor speed	0.192	0.022	7.02	<0.001			
Mean local clustering					0.188	2.24	0.026
Psychomotor speed	0.043	0.021	2.12	0.055			
Lambda (λ)					0.196	2.05	0.042

[a] Models are first corrected for age, sex, mean systolic blood pressure, estimated IQ, and depressive symptoms. Next, the variables of interest are entered in a forward model, first entering the predictor with the highest statistical significance, until no other predictors are statistically significant.
[b] Increase in percentage of the variance explained by the full model including gray matter network properties with respect to the first block including only age, sex, mean systolic blood pressure, estimated IQ, and depressive symptoms.

TABLE VII. Linear forward regression models of global/local clustering and path length with demographic/clinical variables in all patients

	Model characteristics			Association characteristics		
	Adjusted R^2	F-value	P	Standardized β	t-value	P
Mean local path length	0.233	16.16	<0.001			
Age				−0.393	−4.15	<0.001
Retinopathy				−0.191	−2.02	0.047
Mean local clustering	0.321	16.77	<0.001			
Age				−0.255	−3.00	0.003
Gray matter volume				0.491	4.99	<0.001
Sex (being female)				0.467	4.72	<0.001
Small worldness	0.433	26.46	<0.001			
Age				−0.484	−6.40	<0.001
Gray matter volume				0.368	4.86	<0.001
Body mass index				−0.216	−2.87	0.005
Gamma (γ)	0.430	26.17	<0.001			
Age				−0.516	−6.81	<0.001
Gray matter volume				0.317	4.18	<0.001
Body mass index				−0.220	−2.91	0.005
Lambda (λ)	0.408	23.98	<0.001			
Age				−0.570	−7.34	<0.001
Body mass index				−0.188	−2.41	0.018
Sex (being female)				0.158	2.01	0.047
Global clustering	0.330	17.41	<0.001			
Age				−0.291	−3.45	0.001
Gray matter volume				0.480	4.91	<0.001
Sex (being female)				0.440	4.48	<0.001
Global path length	0.248	17.52	<0.001			
Age				−0.476	−5.49	<0.001
Body mass index				−0.178	−2.06	0.042

spatially widespread pattern of correlations with fractional anisotropy, which explained about 33% of the variance. A previous study demonstrated the existence of white matter fiber bundles between cortical regions that show significant positive correlations (i.e. convergence) in thickness [Gong et al., 2012]. Such a relationship between gray matter structure and white matter connectivity was also found in T1DM patients [Franc et al., 2011]. Taken together, it can be hypothesized that white matter alterations underlie cortical network reorganization. We have chosen the TBSS approach over tractography, to explore whether there is any spatial correlation between white matter connections and gray matter network topology. Our results suggest that such a relationship might indeed exist, and for future research we will further investigate the relationship between white matter and gray matter network properties.

For γ and λ differences between patients without proliferative retinopathy and controls reached statistical significance, whereas for non-normalized clustering and path length this trended to be significant. Cohen's δ was lower for non-normalized path length than for λ, with comparable effect sizes for clustering (Table II). This difference suggests that the normalized values, which quantify the network parameters against a random network, are more sensitive in detecting subtle differences and may have more explanatory value in T1DM with and without proliferative retinopathy.

A limitation of the present study is that patients with proliferative retinopathy were, understandably, relatively older, had the earliest onset age, longest disease duration and a higher prevalence of hypertension. It can take up to 15 to 20 years for proliferative retinopathy to develop, if it develops [Klein et al., 1998], and in the presence of microangiopathy (high) blood pressure is likely to be under strict treatment. We could correct our analysis for age and blood pressure. To eliminate the potential effect of diabetes onset and duration differences we repeated the group analysis on a subset of subjects matched for age, diabetes onset age and duration, and yielded similar results as the original analysis, indicating these factors probably did not confound our results. Due to high collinearity of path length and clustering values between various regions, it was not possible to obtain reliable regression models of cognition with regional alterations in network parameters. Therefore we averaged these local measures across the regions that showed alterations between groups. As such we were unable to determine if correlations with cognitive functioning were driven by changes in more specific regions. Our results do however show that both path length and clustering are important for cognitive functioning. The choice to combine the 90
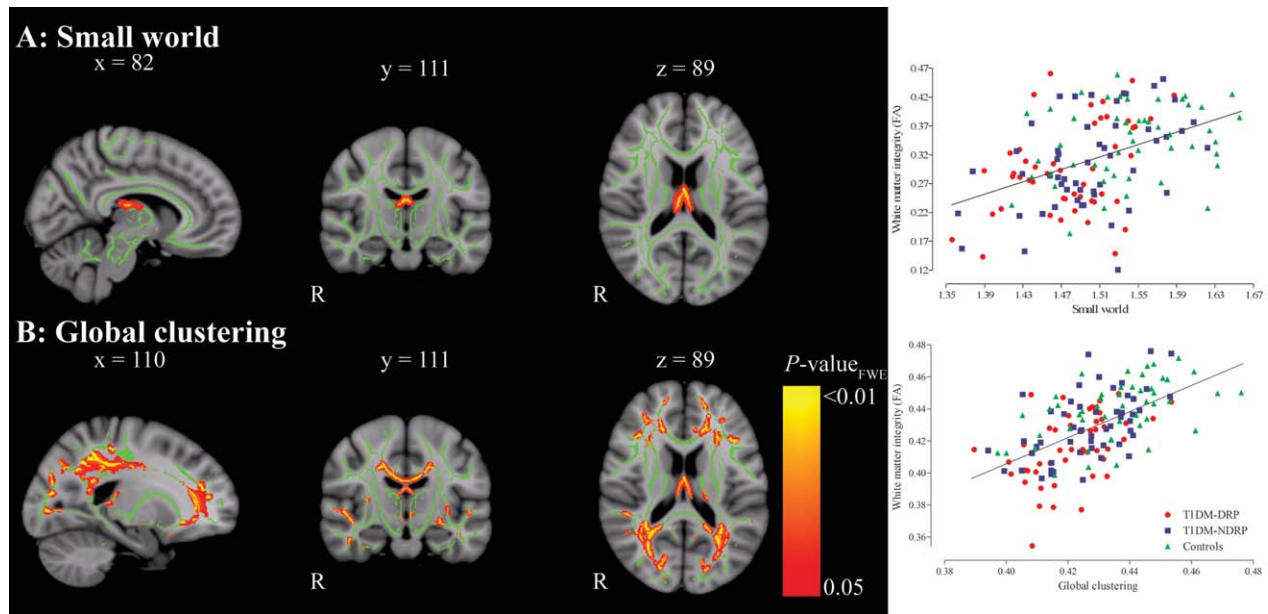
Figure 3.

Schematic representation of the parts of the white matter skeleton that are correlated with small world (**A**) and global clustering (**B**), with the corresponding scatter plots. Areas of a statistically significant correlation after FWE-correction for multiple comparisons are displayed as thickened tracts for visualization purposes. Mean fractional anisotropy value of the significant voxels were extracted and used in the scatterplots. Red circles represent patients with proliferative retinopathy (T1DM-DRP); blue squares represent patients without proliferative retinopathy (T1DM-NDRP) and green triangles represent controls. [Color figure can be viewed in the online issue, which is available at wileyonlinelibrary.com.]

unilateral regions into 45 bilateral regions prevents us from identifying laterality effects. However, this approach was chosen as it significantly reduces the amount of statistical tests that were performed and because network parameters are more robust as they are measured in a larger area. This combined increases the reliability of the results. Global efficiency, which is the inverse of path length, was not added to this study. First, global efficiency is less sensitive to potentially disconnected nodes. Secondly, because all subject-specific networks were fully connected, global efficiency showed a high correlation with path length ($r \geq 0.90$) and was thus redundant. Lastly, we have used fractional anisotropy, derived from DTI-scans, to measure white matter diffusion properties, which may approximate white matter integrity. However, care should be taken when interpreting fractional anisotropy as white matter integrity, because it can be affected by many processes, including methodological, such as crossing fibers, and biological, such as altered fiber coherence, and demyelination processes [Jones et al., 2013].

CONCLUSION

In conclusion, we showed that cortical gray matter organization is more random in T1DM patients both with and without proliferative retinopathy compared with healthy controls. These alterations in cortical networks contain clinically relevant information as they associate with (poorer) cognitive performance beyond the variance explained by classical and T1DM-specific predictors such as age, sex, IQ, and retinopathy. The time-course, underlying mechanisms and predictive value of cortical network reorganization should be determined in future longitudinal studies.

ACKNOWLEDGMENTS

analysis strategy, assisted in the analysis of the data and interpretation of the results. All above-mentioned authors made critical revisions to the manuscript. M.D. was principal investigator of the overall project, designed and supervised the study and obtained funding from the Dutch Diabetes Research Foundation and EFSD for the study. The sponsors had no role in study design, data collection, analysis, interpretation, or writing of the report. E.vD. and B.M.T. had full access to the data and had final responsibility for the decision to submit the article.

REFERENCES

Aldington SJ, Kohner EM, Meuer S, Klein R, Sjølie AK (1995): Methodology for retinal photography and assessment of diabetic retinopathy: The EURODIAB IDDM Complications Study. Diabetologia 38:437–444.

Alemán-Gómez Y, Melie-García L, Valdes-Hernández P. (2006): IBASPM: toolbox for automatic parcellation of brain structures. Presented at: The 12th Annual Meeting of the Organization for Human Brain Mapping, June 11–15, 2006, Florence, Italy. Available on CD-Rom in NeuroImage, Vol. 27, No. 1.

Alexander-Bloch A, Giedd JN, Bullmore E (2013): Imaging structural co-variance between human brain regions. Nat Rev Neurosci 14:322–336.

Bassett DS, Bullmore E, Verchinski BA, Mattay VS, Weinberger DR, Meyer-Lindenberg A (2008): Hierarchical organization of human cortical networks in health and schizophrenia. J Neurosci 28:9239–9248.

Beauquis J, Homo-Delarche F, Revsin Y, De Nicola AF, Saravia F (2008): Brain alterations in autoimmune and pharmacological models of diabetes mellitus: Focus on hypothalamic-pituitary-adrenocortical axis disturbances. Neuroimmunomodulation 15:61–67.

Biessels GJ, Deary IJ, Ryan CM (2008): Cognition and diabetes: a lifespan perspective. Lancet Neurol 7:184–190.

Brands AM, Biessels GJ, de Haan EH, Kappelle LJ, Kessels RP (2005): The effects of type 1 diabetes on cognitive performance: A meta-analysis. Diabetes Care 28:726–735.

Brands AMA, Kessels RPC, Hoogma RPLM, Henselmans JML, van der Beek Boter JW, Kappelle LJ, de Haan EHF, Biessels GJ (2006): Cognitive performance, psychological well-being, and brain magnetic resonance imaging in older patients with type 1 diabetes. Diabetes 55:1800–1806.

Brownlee M (2001): Biochemistry and molecular cell biology of diabetic complications. Nature 414:813–820.

Bullmore E, Sporns O (2012): The economy of brain network organization. Nat Rev Neurosci 13:336–349.

Collin G, van den Heuvel MP (2013): The ontogeny of the human connectome: Development and dynamic changes of brain connectivity across the life span. Neuroscientist 19:616–628.

de Rekeneire N, Peila R, Ding J, Colbert LH, Visser M, Shorr RI, Kritchevsky SB, Kuller LH, Strotmeyer ES, Schwartz AV, Vellas B, Harris TB (2006): Diabetes, hyperglycemia, and inflammation in older individuals. Diabetes Care 29:1902–1908.

Demuru M, van Duinkerken E, Fraschini M, Marrosu F, Snoek FJ, Barkhof F, Klein M, Diamant M, Hillebrand A (2014): Changes in MEG resting-state networks are related to cognitive decline in type 1 diabetes mellitus patients. NeuroImage 5:69–76.

Du Yan S, Zhu H, Fu J, Yan SF, Roher A, Tourtellotte WW, Rajavashisth T, Chen X, Godman GC, Stern D, Schmidt AM (1997): Amyloid-β peptide-receptor for advanced glycation endproduct interaction elicits neuronal expression of macrophage-colony stimulating factor: A proinflammatory pathway in Alzheimer disease. Proc Natl Acad Sci USA 94:5296–5301.

Evans AC (2013): Networks of anatomical covariance. Neuroimage 80:489–504.

Franc DT, Kodl CT, Mueller BA, Muetzel RL, Lim KO, Seaquist ER (2011): High connectivity between reduced cortical thickness and disrupted white matter tracts in longstanding type 1 diabetes. Diabetes 60:315–319.

Gaudieri PA, Chen R, Greer TF, Holmes CS (2008): Cognitive function in children with type 1 diabetes: A meta-analysis. Diabetes Care 31:1892–1897.

Genovese CR, Lazar NA, Nichols T (2002): Thresholding of statistical maps in functional neuroimaging using the false discovery rate. Neuroimage 15:870–878.

Gong G, He Y, Chen ZJ, Evans AC (2012): Convergence and divergence of thickness correlations with diffusion connections across the human cerebral cortex. Neuroimage 59:1239–1248.

Harrison BJ, Pujol J, López-Solà M, Hernández-Ribas R, Deus J, Ortiz H, Soriano-Mas C, Yücel M, Pantelis C, Cardoner N (2008): Consistency and functional specialization in the default mode brain network. Proc Natl Acad Sci USA 105:9781–9786.

He Y, Chen Z, Evans A (2008): Structural insights into aberrant topological patterns of large-scale cortical networks in Alzheimer's disease. J Neurosci 28:4756–4766.

He Y, Chen ZJ, Evans AC (2007): Small-world anatomical networks in the human brain revealed by cortical thickness from MRI. Cereb Cortex 17:2407–2419.

Hughes TM, Ryan CM, Aizenstein HJ, Nunley K, Gianaros PJ, Miller R, Costacou T, Strotmeyer ES, Orchard TJ, Rosano C (2013): Frontal gray matter atrophy in middle aged adults with type 1 diabetes is independent of cardiovascular risk factors and diabetes complications. J Diabetes Complications 27:558–564.

Humphries MD, Gurney K (2008): Network 'small-world-ness': A quantitative method for determining canonical network equivalence. PLoS One 3, e0002051. doi: 10.1371/journal.pone.0002051.

Jacobson AM, Ryan CM, Cleary PA, Waberski BH, Weinger K, Musen G, Dahms W (2011): Biomedical risk factors for decreased cognitive functioning in type 1 diabetes: An 18 year follow-up of the Diabetes Control and Complications Trial (DCCT) cohort. Diabetologia 54:245–255.

Jenkinson M, Smith S (2001): A global optimisation method for robust affine registration of brain images. Med Image Anal 5:143–156.

Jones DK, Knösche TR, Turner R (2013): White matter integrity, fiber count, and other fallacies: The do's and don'ts of diffusion MRI. Neuroimage 73:239–254.

Klein R, Klein BEK, Moss SE, Cruickshanks KJ (1998): The Wisconsin epidemiologic study of diabetic retinopathy: XVII: The 14-year incidence and progression of diabetic retinopathy and associated risk factors in type 1 diabetes1. Ophthalmology 105:1801–1815.

Lyoo IK, Yoon S, Jacobson AM, Hwang J, Musen G, Kim JE, Simonson DC, Bae S, Bolo N, Kim DJ, Weinger K, Lee JH, Ryan CM, Renshaw PF (2012): Prefrontal cortical deficits in type 1 diabetes mellitus: Brain correlates of comorbid depression. Arch Gen Psychiatry 69:1267–1276.

Lyoo IK, Yoon S, Renshaw PF, Hwang J, Bae S, Musen G, Kim JE, Bolo N, Jeong HS, Simonson DC, Lee SH, Weinger K, Jung JJ, Ryan CM, Choi Y, Jacobson AM (2013): Network-level structural abnormalities of cerebral cortex in type 1 diabetes mellitus. PLoS One 8, e71304. doi:10.1371/journal.pone.0071304.

Maslov S, Sneppen K (2002): Specificity and stability in topology of protein networks. Science 296:910–913.

Musen G, Lyoo IK, Sparks CR, Weinger K, Hwang J, Ryan CM, Jimerson DC, Hennen J, Renshaw PF, Jacobson AM (2006): Effects of type 1 diabetes on gray matter density as measured by voxel-based morphometry. Diabetes 55:326–333.

Noble WS (2009): How does multiple testing correction work? Nat Biotechnol 27:1135–1137.

Northam EA, Anderson PJ, Werther GA, Warne GL, Adler RG, Andrewes D (1998): Neuropsychological complications of IDDM in children 2 years after disease onset. Diabetes Care 21: 379–384.

Ouwens DM, van Duinkerken E, Schoonenboom SNM, Herzfeld de Wiza D, Klein M, van Golen L, Pouwels PJW, Barkhof F, Moll AC, Snoek FJ, Teunissen CE, Scheltens P, Diamant M (2014): Cerebrospinal fluid levels of Alzheimer's disease biomarkers in middle-aged patients with type 1 diabetes. Diabetologia 57:2208–2214.

Ownby R (2010): Neuroinflammation and cognitive aging. Cur Psychiatry Rep 12:39–45.

Pezawas L, Verchinski BA, Mattay VS, Callicott JH, Kolachana BS, Straub RE, Egan MF, Meyer-Lindenberg A, Weinberger DR (2004): The brain-derived neurotrophic factor val66met polymorphism and variation in human cortical morphology. J Neurosci 24:10099–10102.

Rubinov M, Sporns O (2010): Complex network measures of brain connectivity: Uses and interpretations. Neuroimage 52:1059–1069.

Sanabria-Diaz G, Melie-García L, Iturria-Medina Y, Alemán-Gómez Y, Hernández-González G, Valdés-Urrutia L, Galán L, Valdés-Sosa P (2010): Surface area and cortical thickness descriptors reveal different attributes of the structural human brain networks. Neuroimage 50:1497–1510.

Smolina K, Wotton CJ, Goldacre MJ (2015): Risk of dementia in patients hospitalised with type 1 and type 2 diabetes in England, 1998–2011: A retrospective national record linkage cohort study. Diabetologia 58:942–950.

Stam CJ (2010): Characterization of anatomical and functional connectivity in the brain: A complex networks perspective. Int J Psychophysiol 77:186–194.

The Diabetes Control and Complications Trial Research Group (1996): Effects of intensive diabetes therapy on neuropsychological function in adults in the diabetes control and complications trial. Ann Intern Med 124:379–388.

Tijms BM, Seriès P, Willshaw DJ, Lawrie SM (2012): Similarity-based extraction of individual networks from gray matter MRI scans. Cereb Cortex 22:1530–1541.

Tijms BM, Möller C, Vrenken H, Wink AM, de Haan W, van der Flier WM, Stam CJ, Scheltens P, Barkhof F (2013): Single-subject gray matter graphs in alzheimer's disease, e58921. PLoS One 8, e58921. doi:10.1371/journal.pone.0058921.

Tijms BM, Yeung HM, Sikkes SA, Möller C, Smits LL, Stam C, Scheltens P, van der Vlier WM, Barkhof F (2014): Single-subject gray matter graph properties and their relationship with cognitive impairment in early- and late onset Alzheimer's disease. Brain Connect. 4:337–346.

Tijms BM, Sprooten E, Job D, Johnstone EC, Owens DGC, Willshaw D, Seriès P, Lawrie SM (2015): Gray matter networks in people at increased familial risk for schizophrenia. Schizophr Res 168:1–8.

Tzourio-Mazoyer N, Landeau B, Papathanassiou D, Crivello F, Etard O, Delcroix N, Mazoyer B, Joliot M (2002): Automated anatomical labeling of activations in SPM using a macroscopic anatomical parcellation of the MNI MRI single-subject brain. Neuroimage 15:273–289.

van Duinkerken E, Klein M, Schoonenboom NS, Hoogma RP, Moll AC, Snoek FJ, Stam CJ, Diamant M (2009): Functional brain connectivity and neurocognitive functioning in patients with longstanding type 1 diabetes mellitus with and without microvascular complications: A magnetoencephalography study. Diabetes 58:2335–2343.

van Duinkerken E, Schoonheim MM, IJzerman RG, Klein M, Ryan CM, Moll AC, Snoek FJ, Barkhof F, Diamant M, Pouwels PJ (2012a): Diffusion tensor imaging in type 1 diabetes: Decreased white matter integrity relates to cognitive functions. Diabetologia 55:1218–1220.

van Duinkerken E, Schoonheim MM, Sanz-Arigita EJ, IJzerman RG, Moll AC, Snoek FJ, Ryan CM, Klein M, Diamant M, Barkhof F (2012b): Resting-state brain networks in type 1 diabetes patients with and without microangiopathy and their relation with cognitive functions and disease variables. Diabetes 61:1814–1821.

van Duinkerken E, Schoonheim MM, Steenwijk MD, Klein M, Ijzerman RG, Moll AC, Heijmans MW, Snoek FJ, Barkhof F, Diamant M (2014): Ventral striatum, but not cortical volume loss is related to cognitive dysfunction in type 1 diabetes patients with and without microangiopathy. Diabetes Care 37: 2483–2490.

van Wijk BCM, Stam CJ, Daffertshofer A (2010): Comparing brain networks of different size and connectivity density using graph theory. PLoS One 5, e13701. doi: 10.1371/journal.pone.0013701.

Watts DJ, Strogatz SH (1998): Collective dynamics of 'small-world' networks. Nature 393:440–442.

Wessels A, Simsek S, Remijnse P, Veltman D, Biessels G, Barkhof F, Scheltens P, Snoek F, Heine R, Rombouts S (2006): Voxel-based morphometry demonstrates reduced gray matter density on brain MRI in patients with diabetic retinopathy. Diabetologia 49:2474–2480.

Wessels AM, Scheltens P, Barkhof F, Heine RJ (2008): Hyperglycaemia as a determinant of cognitive decline in patients with type 1 diabetes. Eur J Pharmacol 585:88–96.

Yates KF, Sweat V, Yau PL, Turchiano MM, Convit A (2012): Impact of metabolic syndrome on cognition and brain: A selected review of the literature. Arterioscler Thromb Vasc Biol 32:2060–2067.